Kinetics of Smelting Reduction of Iron-oxysulfide Slags

Dong-Hwan KIM, Jae-Ki CHOI, Hae-Geon LEE and Jung-Sik KIM
Dong-Hwan Kim and Jae-Ki Choi are research assistants, Hae-Geon Lee is a professor at
Department of Materials Science and Metallurgical Engineering,
Pohang University of Science and Technology(POSTECH)
San 31, Hyoja-dong, Nam-ku, Pohang, 790-784, Korea,
Jung-Sik Kim is a senior researcher at Technical Research Laboratories,
Pohang Iron & Steel Co., Ltd.(POSCO),
P.O.Box 361, Pohang, 790-785, Korea

Key Words: smelting reduction, Fe-O-S melt, iron-oxysulfide, ironmaking, reaction rate, electrochemical reaction

Abstract

A study was undertaken to determine the reduction rate of iron oxide in Fe-O-S melts by solid carbon. It was found that reduction of iron oxide occurred by the direct reaction of solid carbon with iron oxide, and the indirect reduction by CO gas was insignificant. The product of solid iron formed at the carbon surface, and grew towards the melt. The reduction rate reached a maximum value and continued to stay at the value for some length of time, and then exhibited a gradual fall, followed by a constant residual rate. Temperature dependence of the rate was well represented by the Arrhenius equation. The maximum rate showed a first order dependence on the FeO concentration. Solid iron produced at the graphite surface is very low in carbon, showing a ferritic structure. It is concluded that reduction reaction is controlled by chemical reaction at the interface. Electrochemical reaction of $Fe^{2+} + 2e = Fe(s)$ and $O^{2-} + C(s) = CO(g) + 2e$ occurs and is responsible for the major portion of the reduction reaction until the carbon surface has been fully covered by the product iron.

INTRODUCTION

The liquid iron-oxysulfide (Fe-O-S) system has provided a possibility for the development of a novel process for smelting reduction of iron ore[1,2] owing to the existence of an extensive liquid miscibility gap at low temperatures and a low eutectic temperature of 920°C[3-5], its low viscosity and surface tension[2], and fast dissolution rate of wustite and hematite.[2] It is therefore possible to carry out smelting reduction by using the Fe-O-S melt at low temperatures in the range of 1,000 to 1,200°C,[1] and hence the reduction product will be solid iron. The low temperature operation would provide a number of added advantages in that the product would be free from contamination by gangue in the ore, and very low in carbon and sulfur, provided that the oxygen potential is carefully controlled.[1,2] Referring to the Fe-Cu-O-

S phase diagram[6], the use of iron-oxysulfide melt as a smelting reduction medium might also provide a possibility of recycling steel scrap containing high concentrations of copper which cannot be treated through conventional processes. Elliott[1] outlined the possibility of using the iron-oxysulfide system as an iron smelting reduction medium, and, with his coworkers[2], has attempted to experimentally investigate some fundamentals including reduction rates of FeO dissolved in Fe-O-S melts.

An attempt has been made in the present study to determine the reduction rate of iron oxide in Fe-O-S melts using solid carbon, and to elucidate the reduction mechanism at the melt/carbon interface.

EXPERIMENTAL

Figure 1 schematically shows the experimental apparatus. Fe-O-S mixtures were prepared by mixing high purity FeO and FeS in appropriate ratios. A total mass of 393 grams of the mixture were melted in an iron crucible (54mmID x 60mmOD x 250mmL) under the purified argon atmosphere. Most experiments were carried out at 1,200^{o}C, but the temperature for some runs range was raised to 1,300^{o}C to examine the effect of temperature. A graphite rod (20mm in diameter and 200mm in length) capable of rotation and vertical movement was attached to a holder and positioned just above the melt surface. After homogenization of the Fe-O-S melt by holding for 20 minutes at the experimental temperature, and stirring the melt intermittently, the graphite rod was immersed into the melt. Reduction rates were determined by measuring the volumetric flow rate of the exit gases using a mass flow meter. The signal from the mass flow meter was taken at one second intervals, and recorded in a computer. In the case of argon blowing, a graphite rod having a hole (2mm in diameter) in the center was used. The experimental conditions are summarized in Table 1. The melt sample together with the iron crucible was taken out of the furnace and quenched in water immediately after the completion of each experiment. Behavior of precipitation and growth of solid iron during the smelting reduction process was observed from the quenched samples using optical and scanning electron microscopes. The microstructure and properties of the iron produced were analyzed employing optical microscopy, scanning electron microscopy, electron probe microanalysis(EPMA), and microhardness testing.

RESULTS

Figure 2 shows a typical result of the measurement of gas evolution as a function of time. It is seen that the whole process of gas evolution can be divided into a number of stages: the initial increase in the gas evolution rate (Stage I), a constant rate forming a plateau (Stage II) (hereinafter referred to as the maximum rate), the gradual decrease in the rate with time (Stage III), and finally a constant residual rate (Stage IV). Stage I was confirmed to be characteristic of the experimental system employed in the present work through a separate experiment with an empty crucible under otherwise exactly the same conditions as the actual runs. The initial delay until the rate reaches its true value is due to the time required for the exit gas to travel from the furnace tube to the mass flow meter. In order to understand the behavior at the remaining stages (Stage II-IV), the whole crucible assembly was quenched at a number of different time intervals. From the sectioned specimens it was observed that solid iron was produced at the interface between the graphite and the Fe-O-S melt, and was growing towards the melt with time. Some examples of iron grown at the interface are shown in Figure 3. It is clearly seen that solid metallic iron forms on the surface of the graphite rod. It is also seen that, as time lapses, the amount of solid iron increases and hence the fraction of the graphite surface in direct contact with the Fe-O-S melt decreases (Figure 4(a) and (b)).

However, the general observation is that, although the above-mentioned fraction decreased, the gas evolution rate did not fall accordingly, but rather showed a tendency to stay at a constant value for some length of time (Stage II). Once the process has entered Stage III, the area available for direct reaction between the carbon and the melt is left very small (Fig 4(b)). At Stage IV, the area for direct contact between the carbon and the melt is hardly seen, and hence the graphite rod is considered completely surrounded by the solid iron produced as a result of the reduction reaction. In summary, it appears that the fact that the reduction reaction occurs stage-wise is closely related with the availability and the extent of free interface for direct contact between the graphite and the melt. More systematic analysis of this phenomenon is deferred to the discussion section.

The overall reaction between carbon and iron oxide in the Fe-O-S melt can be expressed by the following equation:

$$FeO(melt) + C(s) = Fe(s) + CO(g) \quad (1)$$

where FeO(melt) and C(s) represent FeO in the Fe-O-S melt and solid graphite, respectively. Direct contact between the melt and carbon will warrant the reaction given by Eq(1) to take place. In the literature[7-22] where the reduction of FeO in oxide melts, i.e., slag, by carbon was studied, it has been suggested that the reaction given by Eq(1) might proceed according to the following two steps:

i) At the melt/gas interface

$$FeO(melt) + CO(g) = Fe(s) + CO_2(g) \quad (2)$$

ii) At the carbon/gas interface

$$C(s) + CO_2(g) = 2CO(g) \quad (3)$$

Suppose that the direct reduction of iron oxide by solid carbon represented by Eq(1) is dominant. Then the product iron will be seen to grow at the surface of the graphite rod. On the other hand, if the indirect reduction of iron oxide by carbon monoxide at the surface of gas bubbles represented by Eq(2), iron particles will form on the bubble surface, and then be either dispersed in the Fe-O-S melt or accumulated at the free surface of the melt. In the present study, nearly all of the iron produced was found to grow at the surface of the graphite rod, and iron particles were hardly seen either in the Fe-O-S medium or at the top surface. Figure 4 shows the cross section of the iron crucible one hour after immersion of the graphite rod into the iron Fe-O-S melt (53.4wt% FeO-46.6wt% FeS). It is seen that solid iron completely surrounds the graphite rod and grows towards the melt. No iron particles are seen in the Fe-O-S melt. It can thus be concluded that reduction of iron oxide in the Fe-O-S melt by carbon occurs mainly by the direct reduction reaction given by Eq(1), and the indirect reduction reaction given by Eq(2) hardly occurs in the present experimental conditions.

From the stoichiometry of Eq(1), each mole of CO produced is equivalent to the production of one mole of iron, and it is possible to convert the volumetric flow rate of the off-gas into the molar reduction rate of iron oxide(FeO) using the following simple equation:

$$-\frac{1}{A}\frac{dn_{FeO}}{dt} = \frac{1}{A}\frac{P}{RT}\frac{dV_{CO}}{dt} \quad (4)$$

where A is the interfacial area (m^2), n_{FeO} is the number of moles of FeO reduced (mol), P is the ambient pressure (atm), R is the gas constant (82.057 x 10^{-6} m^3atm $mol^{-1}K^{-1}$), V_{CO} is the volumetric flow rate of CO gas in the exit stream (m^3), and t is time (sec).

In the rest of this paper, the production rate or reaction rate will be given in terms of the number of moles of FeO reduced at a unit interfacial area (m^2) and in a unit time (sec).

Figure 5 shows the effect of temperature given in the form of an Arrhenius type plot on the maximum rate of reduction of iron oxide in the Fe-O-S melts. It can be seen that the temperature effect is well represented by the Arrhenius equation and the activation energy for the reduction reaction of iron oxide in iron-oxysulfide melt(53.4wt%FeO) by graphite is about 190 kJ mol^{-1}. The large value of the activation energy supports the view that the reduction of

iron oxide by solid carbon is controlled at least in part by a chemical reaction at the interface between the carbon and the melt containing iron oxide.

Figure 6 shows the change with time in the reduction rate of iron oxide in Fe-O-S melts of three different compositions. It is seen that the maximum rate increases with increasing FeO concentration in the melt. A plot of the maximum rate against the FeO concentration shows a linear relationship, as seen in Figure 7. The reduction reaction appears to follow first order rate kinetics.

The effect of the interfacial area between the carbon and the Fe-O-S melt was examined by measuring the rate with different immersion depths of the graphite rod into the melt. The results are given in Figure 8. It is seen that the rate increases with increasing the interfacial area, but the rate per unit interfacial area remains constant (see Figure 9). In other words, the reduction rate is directly proportional to the interfacial area.

Figure 10 shows the microstructure of the metallic iron produced on the graphite surface. It is of interest to know that although the metallic iron grows directly on the graphite surface, no pearlitic structure is seen at all. Hardness of the metal measured by using a microhardness tester showed the values of about 100. The above observations support that the structure of the metal is ferritic.

DISCUSSION

The observation of high activation energy tends to rule out the mass transfer in the melt from the candidates of the rate controlling step, and hence the overall rate must be limited by chemical reaction(s) occurring at the interface, as the reaction product(solid iron) forms mostly at the interface. Then the observation that reduction of iron oxide in the Fe-O-S melt by solid carbon occurs by direct reaction between iron oxide and solid carbon supports that the reaction given by Eq.(1) is rate limiting. Now, the task left on hand is to check if all other observations truly support the view that the reaction given by Eq(1) is rate limiting.

If the reaction given by Eq(1) is elementary and also rate limiting, the rate of reduction of iron oxide in the melt can be represented by the following equation:

$$-\frac{1}{A}\frac{dn_{FeO}}{dt} = k_r C_{FeO} \qquad (5)$$

where k_r(m s^{-1}) is the reaction rate constant for Eq(1), A(m^2) is the interfacial area, and C_{FeO}(mol m^{-3}) is the concentration of FeO in the melt.

The above rate equation, Eq.(5), appears to satisfy the observations that the maximum rate shows a first order dependence on the FeO concentration, and that the maximum rate is directly proportional to the geometric interfacial area between the graphite and the melt. In order to determine if Eq(5) also satisfies the rest of the observations that the reduction rate continues to stay at the maximum value for some length of time before gradual fall, followed by a constant residual rate, it is necessary to gain an insight into the interfacial reactions that are possible. Figure 11 schematically shows four different reaction mechanisms which can conceivably occur at the interface.

Mechanism I (Indirect Reduction via Gas Bubbles)

This mechanism has already been ruled out from a candidate as a major reaction that takes place in the present study.

Mechanism II (Chemical Reaction of Eq(1))

If this mechanism is responsible for the major portion of the reduction process, metallic iron will precipitate initially along the line contact of three phases (melt, carbon and gas), and its further growth will occur only at a point contact of four phases (melt, carbon, gas and metal). Although occurrence of this reaction, however slow its rate might be, is quite conceivable, however, the reduction by this mechanism is unlikely to account for the major

proportion of the overall reduction reaction. Furthermore, this mechanism fails to explain the observation (3) in the above summary. According to this mechanism, the area that is occupied by iron product will increase as the reaction proceeds, and hence the fraction of the interfacial sites that are available for the reaction given by Eq(1) decreases with time. Therefore, the overall reaction rate is expected to decrease with time, but the actual observation is different: the overall rate tends to stay at its maximum value for an extended length of time.

Mechanism III (Electrochemical Reactions)

Since the Fe-O-S melt is ionic in nature, and hence the iron oxide in the melt exists in the form of ions, i.e., Fe^{2+} and O^{2-}, the interfacial reaction given by Eq(1) can be assumed to proceed in an electrochemical manner:

Anodic reaction: $O^{2-} + C(s) = CO(g) + 2e$ (6)

Cathodic reaction: $Fe^{2+} + 2e = Fe(s)$ (7)

In this case, the cathodic and anodic reactions do not necessarily have to take place at the same site: Cathodic reaction can occur either at the carbon/melt interface or at the metal/melt interface, or at both interfaces, whereas the anodic reaction proceeds at the contact line of three phases of the melt, carbon and gas. Electrons can freely move through the graphite and metallic iron. If this is the case, and the cathodic reaction is much slower than the anodic reaction, then the occupation of interfacial sites by metallic iron will hardly affect the rate, as long as some sites are left available for the anodic reaction. A probable reaction procedure will then be,

1) The anodic reaction proceeds at some favorable sites at the interface, and generates electrons as well as CO gas.
2) The cathodic reaction occurs over all other sites at the interface, including the sites of the carbon/melt and metal/melt interfaces.
3) Both cathodic and anodic reactions proceed at a steady state, and the overall reaction rate stays at a constant value as long as the sites initially active for the anodic reaction remain unaffected (Stage II in Figure 2).
4) All the sites for the cathodic reaction at the carbon/melt interface have been used up and further cathodic reaction takes place at the sites of the metal/melt interface, and/or by invading the sites for the anodic reaction. As the sites available for the anodic reaction diminish, the overall reaction rate begins to decrease gradually (Stage III in Figure 2).
5) Eventually all the interfacial area has been covered by the product iron, and sites for either cathodic or anodic reaction are no longer available. Carbon for the reduction reaction can only be supplied by diffusion through the metallic iron. The reduction reaction by this carbon is responsible for the residual rate shown in Stage IV.

The above qualitative explanation is well in accord with the observation (3) in the summary and in Figure 2. Next, further examination of the experimental results to see whether they all support this view is in order. Figure 12(a) is the reproduction of Figure 6, but includes all data points obtained at every one second interval, and Figure 12(b) shows the integrated amount of metallic iron production with time. It is seen that for the melt of 45.0wt%FeO Stage II terminates at about 20 minutes after immersion of the graphite rod. It is also seen that, for this time interval, about 1 kg m^{-2} of iron has been produced. The amount of iron produced at termination of Stage II for the melt of 50wt%FeO (about 17 min) is roughly the same as that for the melt of 45wt%FeO. For the melt of 53.4wt%FeO the time at which Stage II terminates is not clear, but in the range of 7 to 11 min, and the amount of iron produced in the corresponding time range is 0.6 – 1 kg m^{-2}. In summary, the amount of iron produced per unit interfacial area by the time when Stage II ends is roughly the same, irrespective of the melt composition and the interfacial area.

In order to explore further evidence that the cathodic reaction, Eq(7), can occur at a different site from that of the anodic reaction, Eq(6), an additional experiment was conducted,

in which the graphite rod was allowed to touch the iron crucible during Stage III. The result is given in Figure 13. It is of interest to notice that metallic iron grows on the wall of the iron crucible. This never happened when the graphite rod did not touch the crucible (Figure 4). The above observation proves that the cathodic reaction actually takes place at the wall of the iron crucible. Recently, Woolley et al[23] studied the reduction kinetics of $CaO\text{-}SiO_2\text{-}Al_2O_3$ slags containing up to 8 wt% FeO, and reported that the reduction of iron oxide from slag by carbon in iron occurs as separate anodic and cathodic reactions; the locations of these reactions may be physically separated by macroscopic distances, and hence the overall reaction is an electrochemical reaction.

In short, existence of Stage II in the change of the reduction rate with time in the present study supports the view that the overall reduction reaction of iron oxide in Fe-O-S melt, Eq(1), occurs, at least partly, in an electrochemical manner represented by Eqs(6) and (7).

Mechanism IV (Reaction with Carbon Diffused through Metallic Iron)

It is of interest to know that the metallic iron produced on the surface of the graphite rod is extremely low in carbon as seen in Figure 16. A question now arises as to how the solid iron which touches the carbon at one side and the Fe-O-S at the other can possibly be very low in carbon. One conceivable postulation is that the dissolution rate of carbon into the iron at the carbon/metal interface is much slower than either the diffusion rate of carbon in the solid iron or the chemical reaction rate between carbon in iron and iron oxide in the melt at the metal/melt interface. If this is the case, the residual rate of reduction at Stage IV shown in Figure 2 is in fact the rate of the reaction between the carbon transported through the solid iron and iron oxide in the melt, the rate-limiting step of which is the dissolution of carbon at the carbon/iron interface.

Using the results given in Figure 6, the carbon dissolution rate is calculated to be 5×10^{-3} mol C m^{-2} s^{-1}. Since the diffusivity of carbon in γ-iron at 1,200°C is known to be about 5×10^{-10} m^2 s^{-1} [24], and the average thickness of solid iron layer on the graphite surface is $70 - 130 \times 10^{-6}$ m (0.6 – 1 kg m^{-2}), the concentration gradient of carbon required to transfer 5×10^{-3} mol C m^{-2} s^{-1} can be calculated using the following Fick's first law equation:

where J_C is the molar flux of carbon in Fe (molC m^{-2} s^{-1}), D_C is diffusivity of carbon in iron, C is the concentration of carbon in iron (mol m^{-3}), x is the diffusion distance (m), and δ is the thickness of the iron layer (m).

Substituting the corresponding values into the equation, the carbon concentration gradient to be established in the iron layer (ΔC) is found to be 700 – 1,300 molC m^{-3} or 0.1 – 0.2 wt%. If the carbon concentration at the metal/melt interface is negligibly low, the carbon content in

$$J_C = -D_C \frac{dC}{dx} \approx -D_C \frac{\Delta C}{\delta} \qquad (8)$$

iron at the carbon/metal interface is mere 0.1 – 0.2 wt%. These low values of carbon concentration warrants the iron product being solid even at the carbon/metal interface, which was actually the case in the present study.

Considering the qualitative agreement of the above analysis with the experimental results, it can be concluded that the reduction of iron oxide by the carbon transferred through the metallic iron layer is operative at Stage II and III, and responsible for the residual rate of reduction at Stage IV.

CONCLUSIONS

A study was undertaken to determine the reduction rate of iron oxide in Fe-O-S melts by solid carbon. The observations are summarized in the following:

1) Reduction of iron oxide in Fe-O-S melts by solid carbon occurs by direct reaction between iron oxide and solid carbon, and the indirect reduction by CO gas is insignificant.
2) The product of the reduction reaction is solid iron, which forms at the interface between the graphite and the melt, and grows towards the melt.
3) On immersion of graphite rod into the melt, the reduction rate reaches a maximum value and continues to stay at the value for some length of time, and then exhibits a gradual fall, followed by a constant residual rate.
4) Temperature dependence of the rate is well represented by the Arrhenius equation, and the activation energy is 190kJ mol^{-1} for 53.4wt% FeO.
5) The maximum rate shows a first order dependence on the FeO concentration, and is directly proportional to the geometric interfacial area between the graphite and the melt.
6) Solid iron produced at the graphite surface is very low in carbon, showing a ferritic structure.

From the experimental results, the following conclusions have been drawn:

1) The reduction reaction is controlled by chemical reaction at the interface.
2) Electrochemical reaction of $Fe^{2+} + 2e = Fe(s)$ and $O^{2-} + C(s) = CO(g) + 2e$ occurs and is responsible for the major portion of the reduction reaction until the carbon surface has fully been covered by the product iron.
3) The dissolution rate of carbon from the graphite rod into the product iron is much slower than either the diffusion rate of carbon in the iron or the reaction rate of iron oxide by carbon diffused in the iron. This results in the product iron being very low in carbon and ferritic in structure.

ACKNOWLEDGMENTS

The authors are thankful to Pohang Iron & Steel Co., Ltd for the financial support for this study.

REFERENCE

1. J.F. Elliott: Proc. Tech. Conf. Proc., 1988, vol. 7, ISS, p109-
2. G.G.K. Murthy and J.F. Elliott: ISIJ Int'l, 1995, vol.34, no.7, p548-554
3. M. Stofko, J. Schmeidl and T. Rosenqvist: Scan. J. Metall., 1974, vol.3, p113-118
4. J.F. Elliott, Met. Trans. B, 1976, vol.7B, p17-33
5. E.T. Turkdogan: "Physico-chemical Properties of Molten Slags and Glasses", The Metal Soc., London, 1983, p224
6. J.F. Elliott: Met. Trans.B, 1976, vol.7B, p17-33
7. F. Fun: Metall. Trans., 1970, vol.1, p2537-41
8. M. Sugata, T. Sugiyama, and K. Kondo: Trans. Iron Steel Inst. Japan, 1974, vol.14, p88-95
9. M. W. Davies, G.S.F. Hazeldean, and P.N. Smith: Proc. Richardson Conf., 1974, p95-107
10. Y. Sasaki and T. Soma: Tetsu-to-Hagane, 1978, vol.64, no.3, p376-384
11. M.P. Shalimov, V.N. Boronenkov, and S.A. Lyamkin: Russ. Metall., 1980, vol.6, p31-34
12. I.D. Sommerville, P. Grieveson, and J. Taylor: Ironmaking Steelmaking, 1980, vol.7, p25-32
13. F. Tsukihashi, M. Amatatsu, and T. Soma: Tetsu-to-Hagane, 1982, vol.68, no.14, p1880-1888
14. H.A. Fine, D. Meyer, D. Janke, and H.J. Engell: Ironmaking Steelmaking, 1985, vol.12, p157-162
15. A. Sato, G. Aragane, K. Kamihira and S. Yoshimatsu: Trans. ISIJ, 1987, vol.27, p789-796
16. S. Hara and K. Ogino: Tetsu-to-Hagane, 1990, vol.76, no.3, p360-367
17. M. Sheikhshab Bafghi, M. Fukuda, Y. Ito, S. Yamada and M. Sano: ISIJ Int'l, 1992, vol.32, p1280-1286
18. D.J. Min and R.J. Fruehan: Metall. Trans.B, 1992, vol.23B, p29-37
19. G.C.K. Murphy, Y. Sawada, and J.F. Elliott: Ironmaking Steelmaking, 1993, vol.20, p179-190
20. M. Sheikhshab Bafghi, M. Fukuda, Y. Ito, S. Yamada and M. Sano: ISIJ Int'l, 1993, vol.33, p1125-1130
21. B. Sarma, A.W. Cramb, and R.J. Fruehan: Met. Mater. Trans.B, 1996, vol.27B, p717-730
22. D.J. Min, J.W. Han, and W.S. Chung: Met. Mater. Trans.B, 1999, vol.30B, p215-221
23. D.E. Wooley and U.B. Pal: Met. Mater. Trans.B, 1999, vol.30B, p877-889
24. L.H. Van Vlack: "Elements of Materials Science and Engineering", 6th Ed., 1959, Addison-Wesley Pub. Co., p207

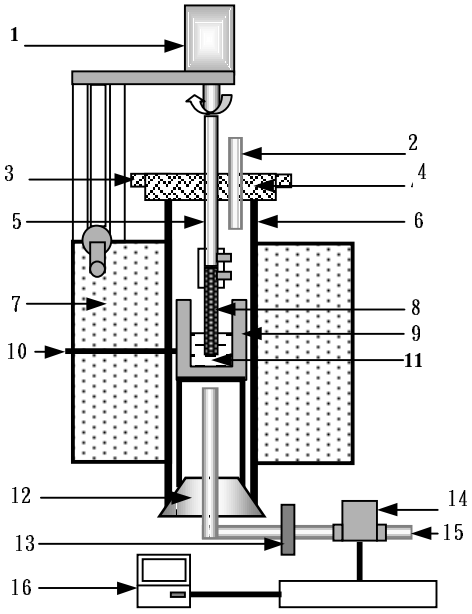

1 DC motor 2 argon gas inlet 3 cooling water 4 brass plate
5 stainless rod 6 mullite tube 7 resistance furnace 8 graphite rod
9 Fe crucible 10 thermocouple 11 Fe-O-S melt 12 silicon rubber
13 Filter 14 Mass Flow Meter 15 gas outlet 16 computer

Fig. 1 Schematic illustration of experimental apparatus

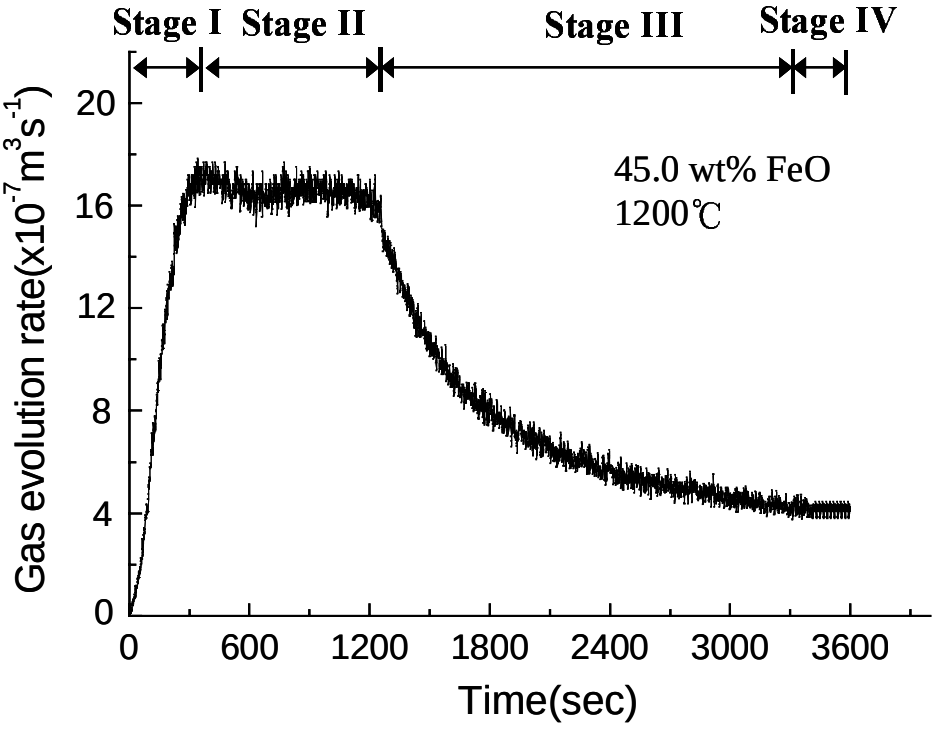

Fig. 2 Change in gas evolution rate with time for reduction of Fe-O-S by graphite (Interfacial area = 3.5_10 -3m2)

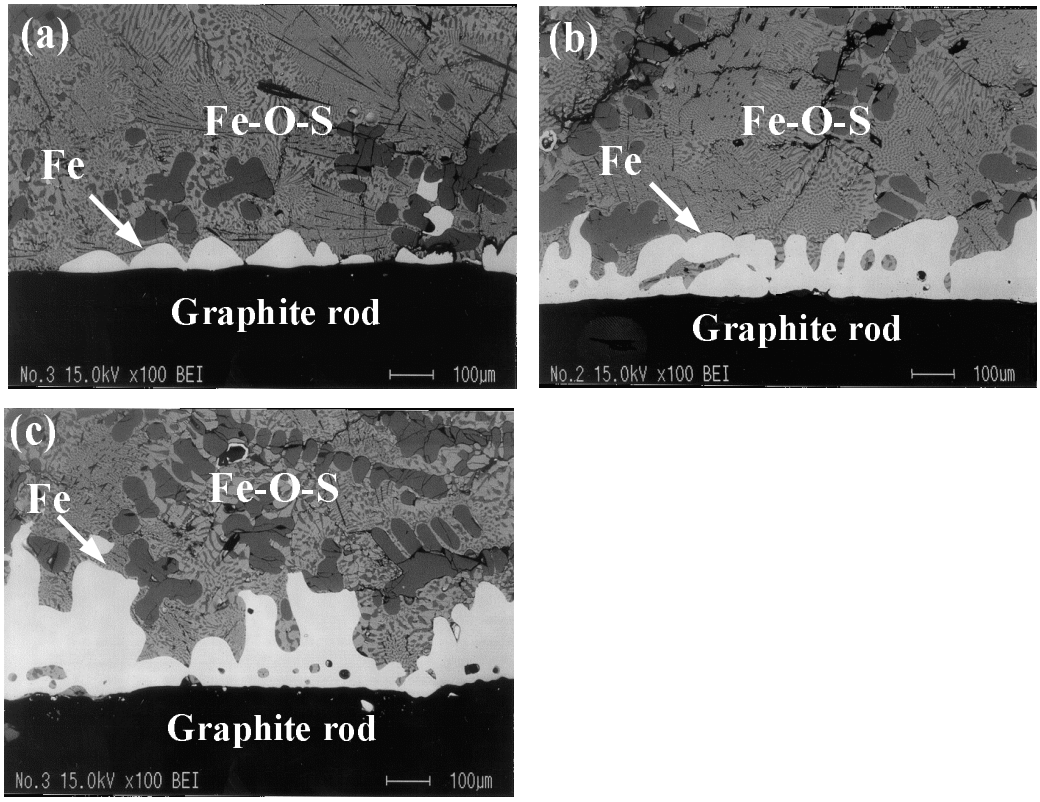

Fig. 3 Solid iron growing at the graphite surface(Initial FeO in slag = 45 wt%): (a) 10 min, (b) 25 min, (c) 60min.

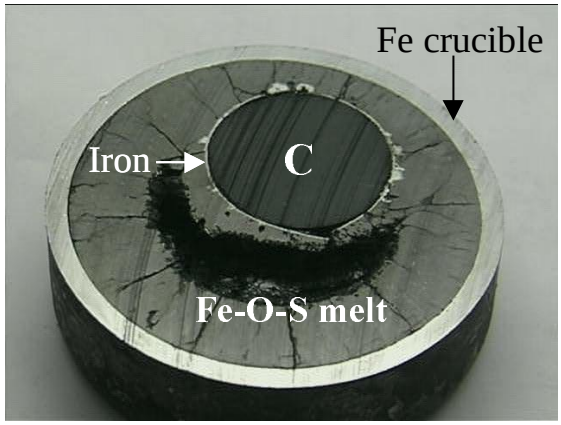

Fig. 4 Cross section of the quenched crucible showing iron product formed around the graphite rod.(1200℃, 53.4 wt% Fe, 1hr)

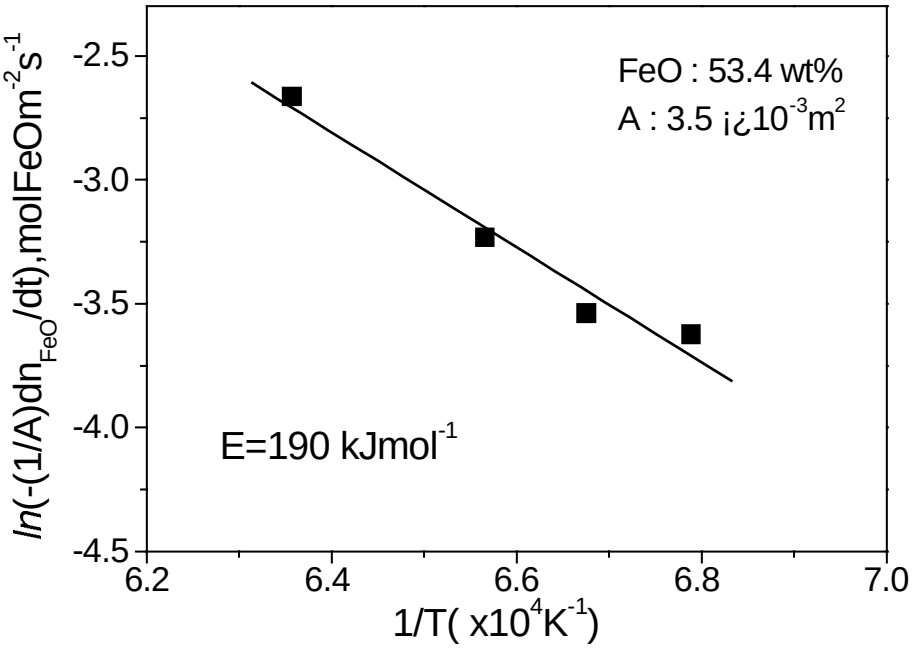

Fig. 5 Arrhenius plot of reduction rate of Fe-O-S melt at different temperatures

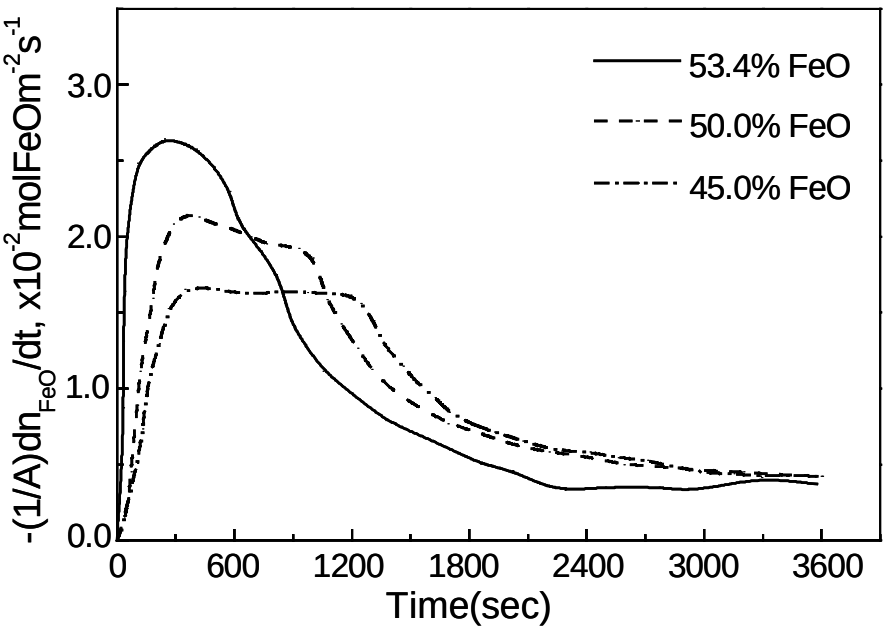

Fig. 6 Change in FeO reduction rate with time at different initial FeO concentrations (1200℃, Area=3.5x10-3m2)

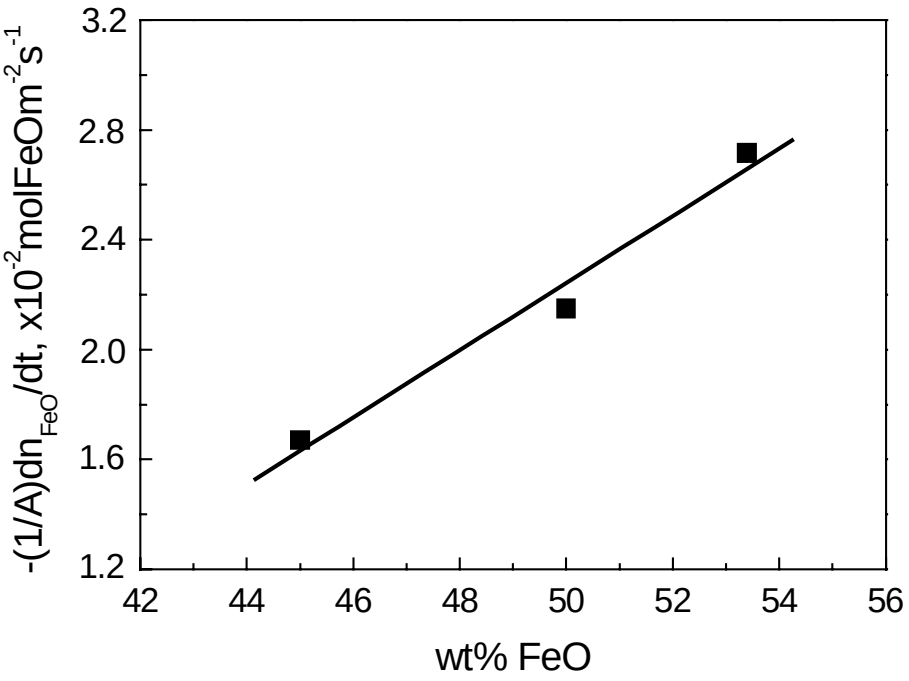

Fig. 7 Effect of FeO concentration on the rate of reduction of FeO (1200℃, Area = 3.5x10-3m2)

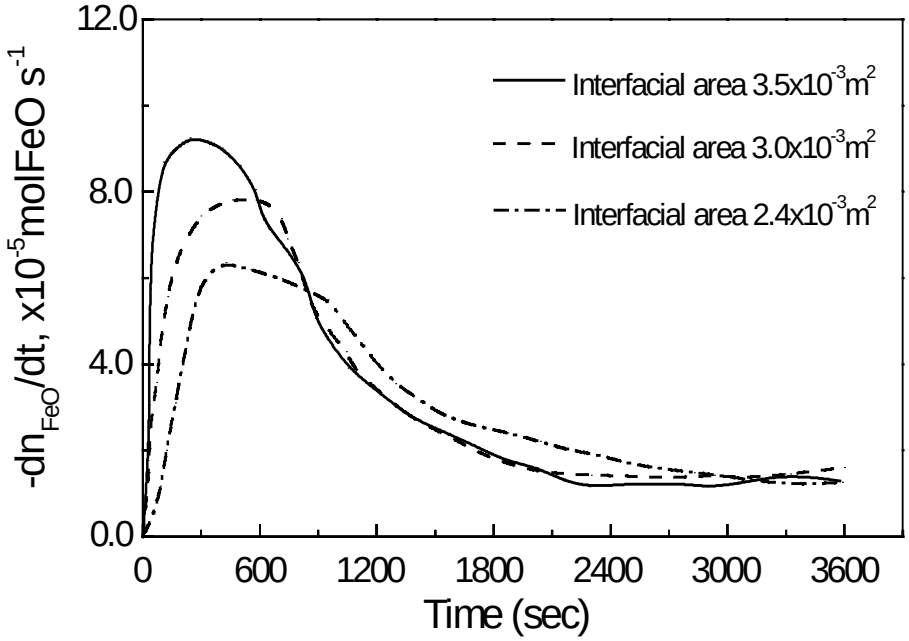

Fig. 8 Change in FeO reduction rate with time at different interfacial reaction areas between graphite rod and melt (1200℃, FeO = 53.4 wt%)

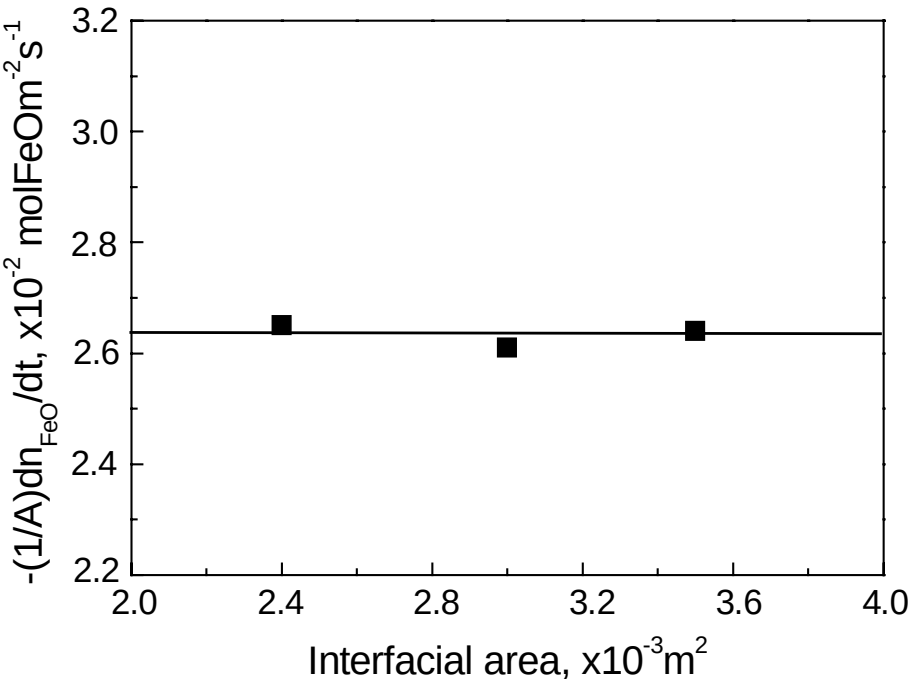

Fig. 9 Effect of interfacial area on the rate of reduction of iron oxide by graphite.(1200℃, 53.4 wt%FeO)

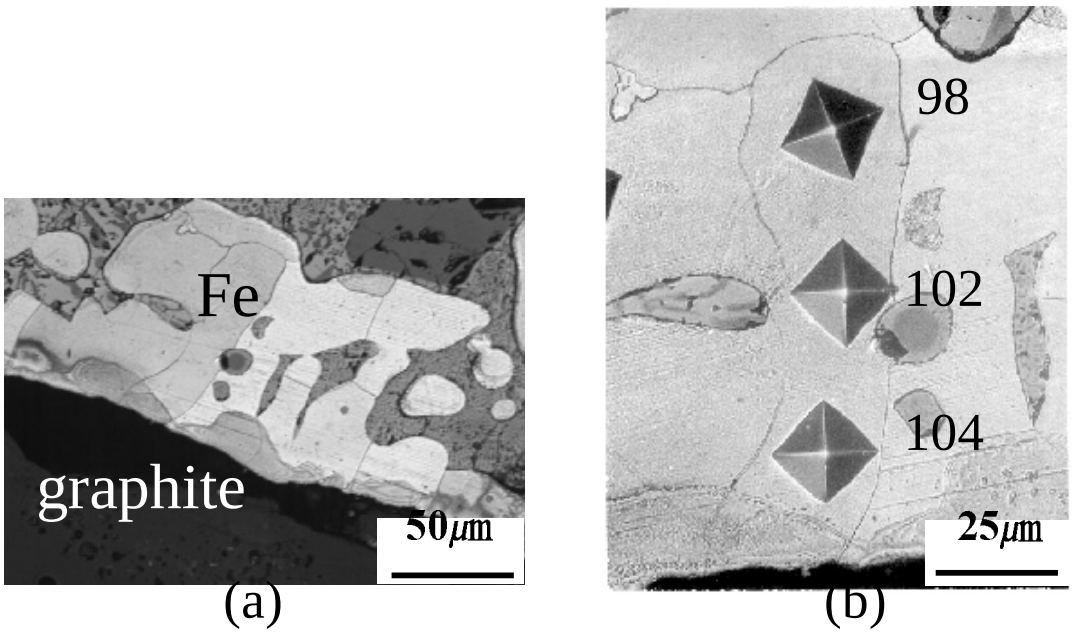

Fig. 10 Microstructure(a) and hardness(b) of iron produced on the graphite surface.(53.4 wt% FeO, 1200℃)

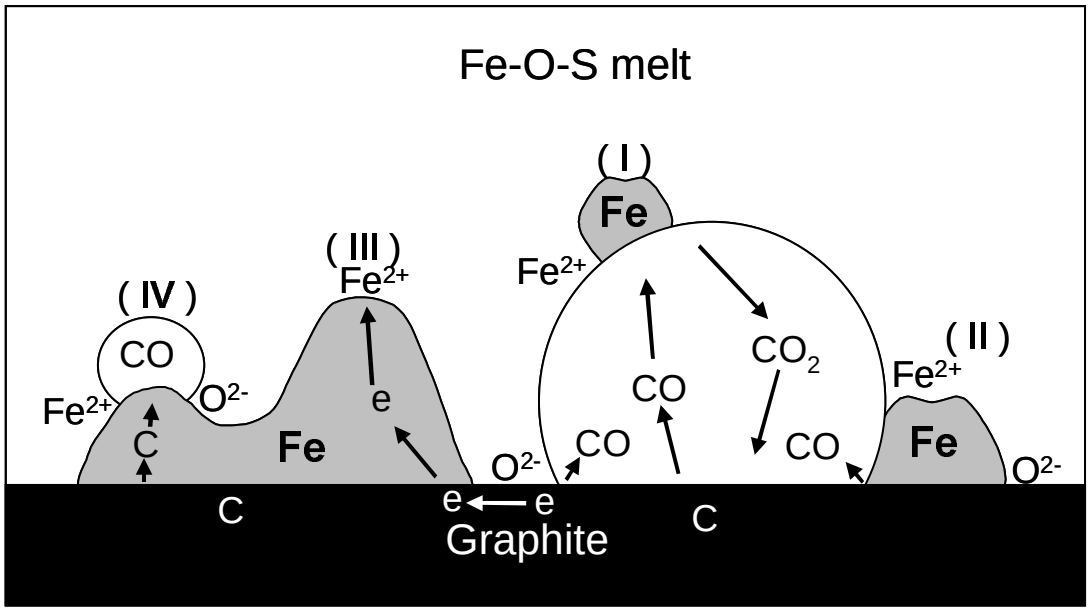

Fig. 11 Four different reaction mechanisms that are conceivable to occur

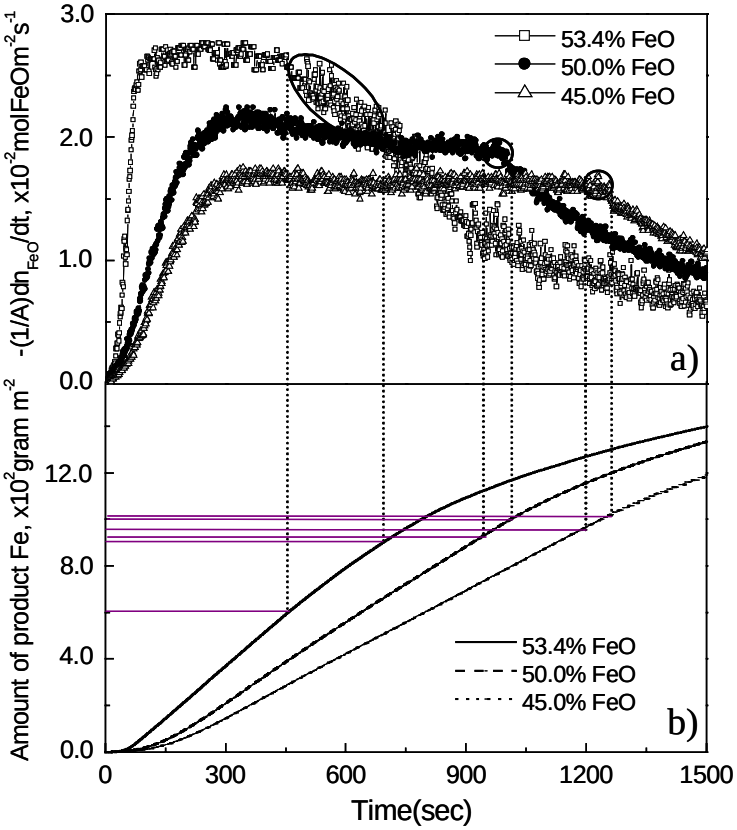

Fig. 12 Change in FeO reduction rate(a) and amount of product Fe(b) with time at different initial FeO concentrations (1200℃, Area=3.5_10-3m2)

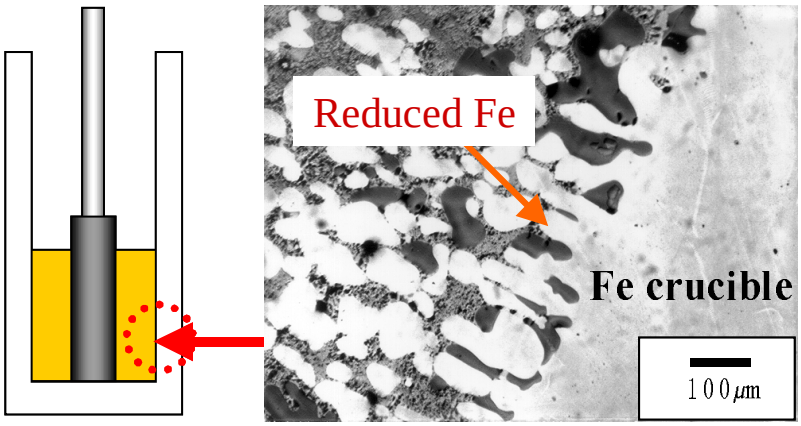

Fig. 13 Reduced Fe at the slag/Fe crucible interface at 1200℃ (initial FeO in melt = 53.4wt%; 3.5_10-3m2)

Table 1 Experimental Conditions in the present study

Effects	Temperature (^{o}C)	FeO (mass%)	Interfacial area (x 10^{-4} m^2)
Reference	1200	53.4	24
Effect of Temperature	1225	53.4	24
	1250	53.4	24
	1300	53.4	24
Effect of composition	1200	45.0	24
	1200	50.0	24
Effect of Interfacial area	1200	53.4	30
	1200	53.4	35